ELSEVIER Chemico-Biological Interactions 119–120 (1999) 99–110

Chemico-Biological Interactions

Theoretical and experimental investigations of electrostatic effects on acetylcholinesterase catalysis and inhibition‘‘

Siobhan Malany [a], Nathan Baker [a], Michelle Verweyst [a], Rohit Medhekar [a], Daniel M. Quinn [a,*], Baruch Velan [b], Chanoch Kronman [b], Avigdor Shafferman [b]

[a] *Department of Chemistry, The University of Iowa, Iowa City, IA, 52242 USA*
[b] *Israel Institute for Biological Research, Ness-Ziona 70450, Israel*

Abstract

The role of electrostatics in the function of acetylcholinesterase (AChE) has been investigated by both theoretical and experimental approaches. Second-order rate constants ($k_E = k_{cat}/K_m$) for acetylthiocholine (ATCh) turnover have been measured as a function of ionic strength of the reaction medium for wild-type and mutant AChEs. Also, binding and dissociation rate constants have been measured as a function of ionic strength for the respective charged and neutral transition state analog inhibitors *m*-(*N*,*N*,*N*-trimethylammonio)trifluoroacetophenone (TMTFA) and *m*-(*t*-butyl)trifluoroacetophenone (TBTFA). Linear free-energy correlations between catalytic rate constants and inhibition constants indicate that k_E for ATCh turnover is rate limited by terminal binding events. Comparison of binding

Abbreviations: AChE, acetylcholinesterase; aM, attomolar = 10^{-18} M; ATCh, acetylthiocholine; DTNB, 5,5′-dithiobis(2-nitrobenzoic acid); D74N, aspartate-74 to asparagine mutant of mouse AChE; D280V, aspartate-280 to valine mutant of mouse AChE; D283N, aspartate-283 to asparagine mutant of mouse AChE; EA, enzyme-substrate complex; EI, enzyme–inhibitor complex; E199Q, glutamate-199 to glutamine mutant of *T. californica* AChE; E202A, glutamate-202 to alanine mutant of human AChE; E202Q, glutamate-202 to glutamine mutant of human AChE; E450A, glutamate-450 to alanine mutant of human AChE; E450Q, glutamate-450 to glutamine mutant of mouse AChE; Glu, glutamic acid; His, histidine; I444, isoleucine-444 of *T. californica* AChE; Ser, serine; TBTFA, *m*-(*t*-butyl)trifluoroacetophenone; TMTFA, *m*-(*N*,*N*,*N*-trimethylammonio)trifluoroacetophenone.

* Corresponding author. Tel. + 1-319-3351335; fax: + 1-319-3351270.
E-mail address: danielquinn@uiowa.edu (D. Quinn)

PII: S0009-2797(99)00018-6

rate constants for TMTFA and TBTFA attests to the sizable electrostatic discrimination of AChE. Free energy profiles for cationic ligand release from the active sites of wild-type and mutant AChEs have been calculated via a model that utilizes the structure of *T. californica* AChE, a spherical ligand, and energy terms that account for electrostatic and van der Waals interactions and chemical potential. These calculations indicate that EA and EI complexes are not bound with respect to electrostatic interactions, which obviates the need for a 'back door' for cationic ligand release. Moreover, the computed energy barriers for ligand release give linear free-energy correlations with $\log(k_E)$ for substrate turnover, which supports the general correctness of the computational model.

Keywords: Acetylcholinesterase; Catalysis; Electrostatics; Ligand diffusion; Transition state; Analog binding

1. Introduction

Acetylcholinesterase is an enzyme that is noted for its pronounced catalytic power. Consistent with this, for acetylcholine hydrolysis the turnover number k_{cat} is $\sim 10^4\ s^{-1}$ and the second-order rate constant $k_E\ (= k_{cat}/K_m)$ is $\sim 10^8\ M^{-1}\ s^{-1}$ [1], a value that is not greatly different than the speed limit of biological catalysis estimated by Eigen and Hammes [2]. Moreover, various investigators have provided experimental evidence that AChE catalysis [3,4] and cationic ligand binding [5,6] are diffusion-controlled processes. However, the X-ray structure of *Torpedo californica* AChE provided a considerable surprise [7], in that the Ser–His–Glu catalytic triad of the active site is near the bottom of a narrow, 20-Å deep gorge that is predominantly lined with the sidechains of aromatic amino acids. This unusual active site architecture in an enzyme of such finely honed catalytic power prompted a flurry of novel experimental and theoretical investigations. Among them were theoretical calculations that indicated that AChE possesses an asymmetric electrical field whose large dipole moment is aligned with the axis of the active site gorge [8]. Brownian dynamics simulations support the idea that the electrical field of AChE accelerates the binding of cationic ligands to the active site [9–11]. This model is supported by the observations that second-order rate constants for binding of conformationally constrained cationic ligands, such as TMTFA [11] and *N*-methylacridinium [6], are sensitive to the ionic strength of the reaction medium and, at zero ionic strength, markedly exceed the Eigen speed limit for biological catalysis [2]. The accelerative effect of the electrical field on cationic ligand binding has led researchers to wonder how the cationic choline product of catalysis can escape from the active site. From this has arisen the anthropomorphic 'back-door' mechanism for product release [12]; this postulate loses sight of the fact that the potential energy change that accompanies separation to infinite distance of choline and AChE is independent of the pathway that the separation takes.

The electrostatic guidance mechanism outlined in the preceding paragraph is not without controversy. Site-specific mutagenesis of multiple charged residues on the

face of human AChE that contains the active site gorge contracts the negative potential to the surface of the enzyme, yet has only modest effects on k_E for hydrolysis of the substrate acetylthiocholine (ATCh) [13]. Theoretical calculations, however, indicate that in the multiply mutated enzyme the gradient of the electrostatic potential in the active site is preserved, and, therefore, one does not expect much of an effect on k_E [9,14]. On the other hand, binding of the cationic snake venom toxin fasciculin to the peripheral anionic site at the opening of the active site gorge of mouse AChE is markedly sensitive both to ionic strength and to neutralization by site-specific mutagenesis of anionic surface residues [11]. Therefore, the importance of the electrostatic guidance mechanism in accelerating the binding of cationic ligands to the peripheral site is unquestioned, but the role of electrostatics in diffusion of cationic substrates to the active site is an issue that is far from settled. The experimental and theoretical approaches that are described below not only bring into harmony the seemingly disparate observations on electrostatic effects in ligand binding versus substrate turnover, but also obviate the need for a 'back door' for release of cationic products.

2. Materials and methods

2.1. Reagents and enzymes

ATCh chloride, DTNB, $NaH_2PO_4 \cdot H_2O$, $Na_2HPO_4 \cdot 7H_2O$ and Type V-S *Electrophorus electricus* AChE were purchased from Sigma (St. Louis, MO, USA). Water used for buffer preparation was distilled and then deionized by passage through a Barnstead D8922 mixed-bed ion-exchange column (Sybron, Dubuque, IA, USA). NaCl was purchased from EM Science (Cherry Hill, NJ, USA). The transition state analog inhibitors TMTFA and TBTFA were synthesized and characterized as described by Nair et al. [15,16]. Wild-type and mutant recombinant AChEs from *T. californica* [17], mouse [18,19] and *Homo sapiens* [20,21] were produced and characterized as described previously.

2.2. Enzyme kinetics

Initial rates of AChE-catalyzed hydrolysis of ATCh were measured in sodium phosphate buffers at pH 7.3–7.4 and 25 ± 0.2°C by the colorimetric, DTNB-coupled Ellman assay [22]. The Michaelis-Menten parameters k_{cat} and K_m were calculated by fitting initial velocity versus substrate concentration data to Eq. (1) [19]:

$$v_i = \frac{k_{cat}[E_T][A](1 + \beta[A]/K_{AA})}{(K_m + [A])(1 + [A]/K_{AA})}. \quad (1)$$

This equation accounts for substrate activation or inhibition at substrate concentrations $[A] \gg K_m$. Rate constants for TMTFA and TBTFA binding to and release from the AChE active site were determined as described by Nair et al. [23].

Dependences of rate constants on ionic strength were fit to Eq. (2), as described by Quinn et al. [24]:

$$k_\mu = (k^0 - k^H)10^{-1.08|Z_E Z_I|\sqrt{\mu}} + k^H \quad (2)$$

In this equation k_μ is the observed rate constant at ionic strength μ, k^0 and k^H are the least-squares values of the rate constant at zero and high ionic strengths, respectively, and z_E and z_I are the respective charges of the enzyme and the ligand. An equation that is similar in form was used to fit dependences of inhibitor dissociation constants (K_i values) on ionic strength.

2.3. Theoretical free energy calculations

Fig. 1 depicts the features of a model that was used to calculate free energy profiles for cationic ligand release from the active site of AChE. The model utilized the coordinates of the structure of *T. californica* AChE and initially situated a spherical ligand in the bottom of the active site gorge. Hydrogens were added to the AChE structure and their positions minimized by using the molecular mechanics package CHARMM22 [25]. The progress of ligand movement up the active site gorge was mapped in a series of discrete steps that increase the distance between the center of the ligand and the Cδ atom of I444. The path of lowest potential energy

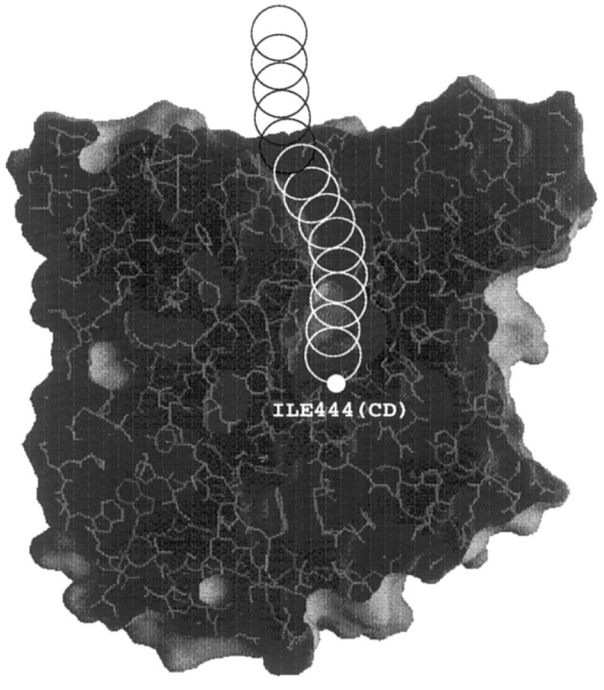

Fig. 1. Pictorial representation of the theoretical model used for computation of the minimum free energy pathway for release of a cationic ligand from the active site of AChE.

from the bottom of the gorge was determined by evaluating the energies of grid elements on a sphere that surrounds the ligand position at each step. For these calculations the partial charges, van der Waals radii and van der Waals well depths were assigned to AChE atoms from the CHARMM22 parameter files. The step size for the path up the gorge was set to either 1 or 2.5 Å and a ligand van der Waals radius of 7 Å was used. The total energy at each grid point on the sphere was calculated as the sum of electrostatic, van der Waals and constraint energies given, respectively, by Eqs. (3)–(5):

$$E_{\mathrm{elec},i} = k \sum_{j=1}^{N} \frac{q_{\mathrm{L}} q_j}{\varepsilon r_{ij}}, \tag{3}$$

$$E_{\mathrm{vdw},i} = \sum_{j=1}^{N} \sqrt{\sigma_{\mathrm{L}} \sigma_j} \left[\left(\frac{R_{\mathrm{L}} + R_j}{2 r_{ij}} \right)^{12} - 2 \left(\frac{R_{\mathrm{L}} + R_j}{2 r_{ij}} \right)^{6} \right], \tag{4}$$

$$E_{\mathrm{cons},i} = k_0 \frac{r_{i,\mathrm{ref}} - r_{\mathrm{ref},0}}{r_0}. \tag{5}$$

In Eq. (3) q_{L} and q_j are the respective charges of the ligand (i.e. $+1$e) and the jth protein atom, r_{ij} is the distance between the ith grid point and the jth protein atom, and the constant $k = 332.0716$ kcal mol^{-1} e^{-1} gives energies in the desired units. The dielectric constant ε was scaled with distance by multiplying an initial dielectric constant of 4 by the distance between the interacting atoms. This scaling takes into account the inhomogeneous dielectric of the protein and the high dielectric of the surrounding solvent. In Eq. (4) R_{L} and R_j are the van der Waals radii of the ligand and the jth protein atom, $\sigma_{\mathrm{L}} = -0.08$ kcal mol^{-1} is the van der Waals well depth of the ligand, and σ_j is the van der Waals well depth of the jth protein atom. The constraint potential in Eq. (5) models the effect of entropy of dilution on ligand release. In this equation k_0 is a weighting factor in kcal mol^{-1}, r_0 is the step size of the simulation, and $r_{i,\mathrm{ref}}$ or $r_{ref,0}$ is the distance between Cδ of I444 and the ith grid point or the center of the sphere. The ligand consistently moved out the active site gorge and into 'bulk solution' for chemical potential weighting factors of 5 kcal mol^{-1} and ligand van der Waals radii greater than 3 Å. The scaling in Eq. (5) ensures a constant driving force at all distances from the bottom of the active site gorge.

The grid point with the lowest total energy was chosen as the center of the next sphere in the ligand release pathway. However, for all steps beyond the first, the potential energy grid was mapped on the sphere but excluding a 30° cone that faces the direction of the previous step. This procedure forces the ligand to move forward, even if the move is to a position that is less favorable energetically than the preceding position, and thereby allows the ligand to surmount energy barriers along the release path. After the new ligand position was chosen, a 30° cone around the new point was evaluated as a 20×20 grid of energy points. The resulting 400 energies approximate a canonical ensemble, from which the partition function at the nth discrete step along the ligand release path was calculated:

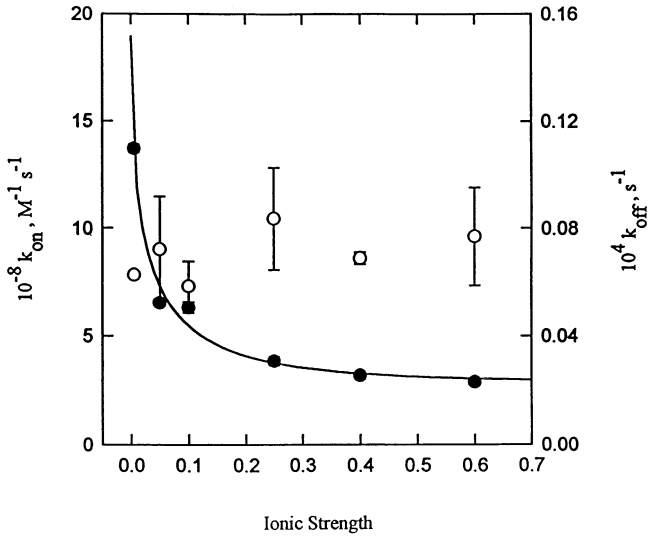

Fig. 2. Ionic strength dependence of the rate constants for interaction of TMTFA with the active site of human AChE. Binding rate constants (k_{on}) and release rate constants (k_{off}) are plotted as solid and open circles, respectively.

$$Q_n = \sum_i e^{-E_i/RT}. \quad (6)$$

The constraint energy is not modeled into the free energy, thereby creating free energy reaction profiles that are independent of the driving force used to create them. Gibbs free energy changes at each of the n distances along the ligand release path were calculated according to Eq. (7):

$$\Delta G_n = -RT(\ln Q_n - \ln Q_{ref}). \quad (7)$$

Q_{ref} is the partition function of the ensemble at the reference point of the pathway, the Cδ of I444. Free energy changes calculated by Eq. (7) are actually Helmholtz free energy differences; however, differences are slight between Helmholtz and Gibbs free energy changes for processes in condensed phases, such as in aqueous solution.

3. Results and discussion

Fig. 2 shows the dependences on ionic strength of the rate constants for binding of TMTFA to the active site of human AChE (k_{on}) and for dissociation of the resulting EI complex (k_{off}). Least-squares fitting of the k_{on} data indicate that the cationic ligand binds to AChE about an order of magnitude faster at zero than at high ionic strength; i.e. $k_{on}^{H} = 1.9 \pm 0.2 \times 10^9$ M^{-1} s^{-1} and $k_{on}^{0} = 2.9 \pm 0.6 \times 10^8$ M^{-1} s^{-1}. Since increasing ionic strength increasingly masks the electrical field of

AChE, the dependence of k_{on} on ionic strength supports the notion that cationic ligand binding is accelerated by the electrical field. However, the rate constant for release of TMTFA from the active site (k_{off}) is insensitive to changes in ionic strength. This observation indicates that the electrical field of AChE has no effect on the release of cationic ligands from the active site of the enzyme, as previously suggested [24]. For the neutral isosteric transition state analog inhibitor TBTFA, increasing ionic strength increases the binding rate constant k_{on} (data not shown), a trend that is opposite to that for TMTFA binding. The effect of ionic strength on TBTFA binding is not surprising, since hydrophobic solutes are salted out of aqueous solution by high concentrations of NaCl. Therefore, the opposite effects of ionic strength on TMTFA and TBTFA binding masks the intrinsic electrostatic discrimination of the enzyme for cationic versus neutral ligands. However, this problem is circumvented when one compares the least-squares extrapolated k^0_{on} values at zero ionic strength.

Table 1 contains k^0_{on} and K^0_i values for TMTFA binding and ratios of k^0_{on} values for TMTFA versus TBTFA. These data are noteworthy for three reasons: (a) k^0_{on} values for TMTFA binding are large for all AChEs studied. For the enzymes from *T. californica*, *E. electricus* and mouse, k^0_{on} values exceed the Eigen limit [2] by an order of magnitude. The only sensible interpretation of these large k^0_{on} values is that binding of TMTFA is a diffusion-controlled process. (b) AChE shows a large discrimination for binding of cationic TMTFA versus neutral TBTFA. Steric effects do not complicate this comparison, since the two transition state analogs are isosteric. This large discrimination is a sure sign of the prominent role of electrostatics in binding of cationic ligands to AChE. (c) TMTFA binds very tightly to AChE, as reflected by values of the inhibitor dissociation constant K^0_i. Affinity is greatest for the *E. electricus* enzyme, which has a K^0_i value of 460 aM.

The linear-free energy correlations of Fig. 3 further explore the role of electrostatics in AChE catalysis. Fig. 3A shows that there is a surprisingly good correlation for $k^0_E(=k_{cat}/K_m$ for ATCh hydrolysis at zero ionic strength) and k^0_{on} for transition state analog binding. This correlation obtains for native and mutant AChEs from diverse species. However, the slope of the correlation is 0.4, which indicates that catalysis is considerably more sensitive than transition state analog

Table 1
Rate and equilibrium constants for interaction of transition state analog inhibitors with wild-type acetylcholinesterases

AChE	TMTFA parameters		$\frac{k^0_{on}(\text{TMTFA})}{k^0_{on}(\text{TBTFA})}$
	$10^{-9}\ k^0_{on}$ ($M^{-1}\ s^{-1}$)	K^0_i (fM)	
Human	1.9 ± 0.2	3.3 ± 0.5	2700 ± 500
Mouse	16 ± 1	1.1 ± 0.3	
T. californica	15 ± 1	9.8 ± 0.8	$22\,000 \pm 200$
E. electricus	18 ± 1	0.460 ± 0.004	5000 ± 700

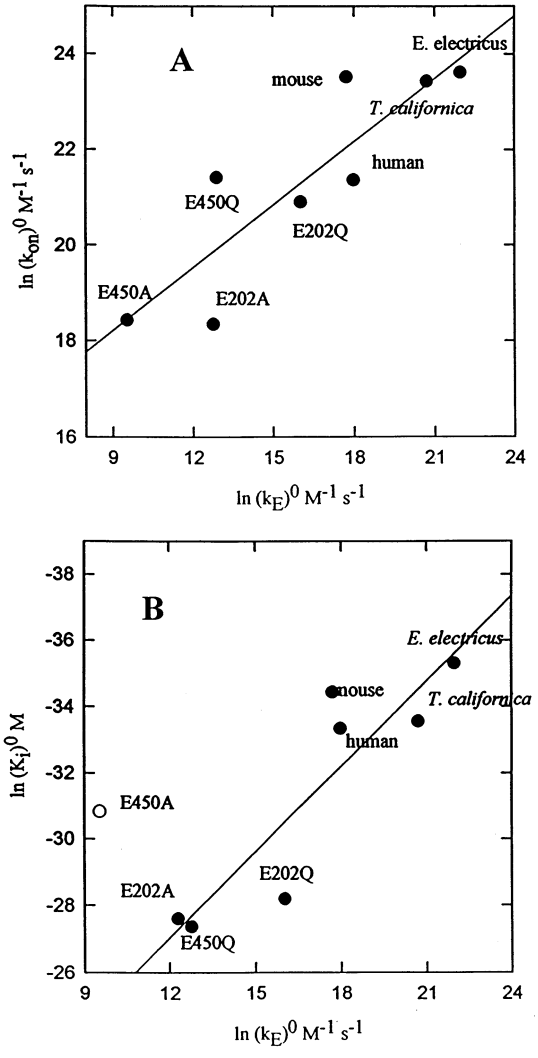

Fig. 3. Linear free-energy correlations for catalysis and inhibition of wild-type and mutant AChEs. (A) Correlation of $\ln(k^0_{on})$ and $\ln(k^0_E)$, where k^0_E is the value of k_{cat}/K_m at zero ionic strength. Linear regression analysis of the correlation gives a slope $= 0.4 \pm 0.1$ and $r = 0.87$. (B) Correlation of $\ln(K^0_i)$ and $\ln(k^0_E)$; linear regression analysis of the correlation gives a slope $= -0.9 \pm 0.2$ and $r = 0.91$. The point for the E450A mutant of human AChE was excluded from the analysis since the effect of this mutation is primarily a reduction in k_{cat}, a rate constant that monitors events after the substrate has bound to the active site of the enzyme.

binding to enzyme variation. Fig. 3B shows that there is also a good correlation between k^0_E and K^0_i, the dissociation constant of the AChE-TMTFA complex. In this case the slope is -0.9, which indicates that catalysis and equilibrium dissociation of the transition state analog complex have essentially the same sensitivity to

enzyme variation. Since K_i^0 depends on the free energy difference between the EI complex and the E + I state, this correlation indicates that the transition state for k_E of ATCh turnover resembles the EI complex. A reasonable interpretation of these observations is that k_E is not prominently rate limited by diffusion to the surface of the enzyme, or from the enzyme surface to the active site, but rather is rate limited by terminal binding events. These could include insertions of the carbonyl oxygen, the acetyl methyl and the quaternary ammonium functions into their respective binding sites, and/or conformational transitions of the substrate to the fully extended conformation [26,27].

Fig. 4 shows computed free-energy profiles for release of a spherical cationic ligand from the active sites of native and mutant AChEs. An important feature of these profiles is that there is an energy barrier at ~ 7–10 Å from Cδ of I444. This barrier arises from both van der Waals (i.e. steric) and electrostatic contributions. Of considerable interest, the position of the barrier corresponds to the position of binding of TMTFA in the transition state analog complex [26], and of acetylcholine in a model of the tetrahedral intermediate of the catalytic mechanism [7]. Therefore, active site complexes of cationic ligands are dissipative with respect to long-range electrostatic interactions, cationic ligands such as choline are not trapped by the electrical field of AChE, and there is no need for a 'back door' for their release. Fig. 5 shows that there is linear free-energy correlation between the computed free-energy barriers for ligand release (and by microscopic reversibility for ligand binding) and k_E^0 for turnover of ATCh. This correlation supports the efficacy of the computational approaches described herein for theoretical calculation of ligand binding and release energetics, and indicates that conclusions drawn from the computed energetics are applicable to the catalytic function of AChE.

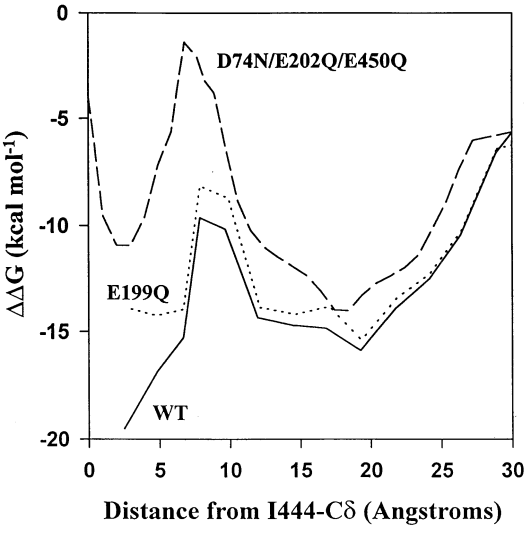

Fig. 4. Calculated free-energy profiles for cationic ligand release from the active sites of wild type and mutant AChEs.

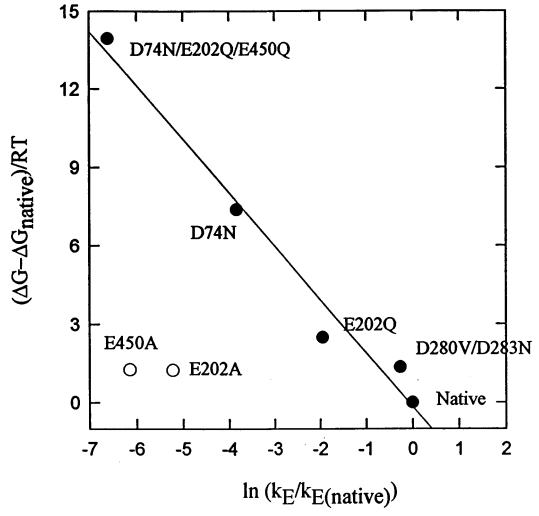

Fig. 5. Linear free-energy correlation between calculated free energies of cationic ligand binding and ln (k_E^0) for hydrolysis of ATCh. The points for the E202A and E450A mutants were excluded from the analysis because the primary effects of the mutations are reductions in k_{cat}.

Acknowledgements

This work was support by NIH grants NS21334 to DMQ, and by US Army Research and Development contract DAMD17-96-C-6088 to AS. SM acknowledges the support of an NIH Biotechnology Predoctoral Training Grant (1T32 GM08365).

References

[1] D.M. Quinn, Acetylcholinesterase: enzyme structure, reaction dynamics, and virtual transition states, Chem. Rev. 87 (1987) 955–979.
[2] M. Eigen, G.G. Hammes, Elementary steps in enzyme reactions, Adv. Enzymol. Relat. Sub. Biochem. 25 (1963) 1–38.
[3] M. Bazelyansky, E. Robey, J.F. Kirsch, Fractional diffusion-limited component of reactions catalyzed by acetylcholinesterase, Biochemistry 25 (1986) 125–130.
[4] B.B. Hasinoff, Kinetics of acetylcholine binding to electric eel acetylcholinesterase in glycerol/water solvents of increased viscosity. Evidence for a diffusion-controlled reaction, Biochim. Biophys. Acta 704 (1982) 52–58.
[5] T.L. Rosenberry, E. Neumann, Interaction of ligands with acetylcholinesterase. Use of temperature-jump relaxation kinetics in the binding of specific fluorescent ligands, Biochemistry 16 (1977) 3870–3878.
[6] H.J. Nolte, T.L. Rosenberry, E. Neumann, Effective charge on acetylcholinesterase active sites determined from the ionic strength dependence of association rate constants with cationic ligands, Biochemistry 19 (1980) 3705–3711.
[7] J.L. Sussman, M. Harel, F. Frolow, C. Oefner, A. Goldman, L. Toker, I. Silman, Atomic structure of acetylcholinesterase from *Torpedo californica*: a prototypic acetylcholine-binding protein, Science 253 (1991) 872–879.

[8] D.R. Ripoll, C.H. Faerman, P.H. Axelsen, I. Silman, J.L. Sussman, An electrostatic mechanism for substrate guidance down the aromatic gorge of acetylcholinesterase, Proc. Natl. Acad. Sci. USA 90 (1993) 5128–5132.
[9] J. Antosiewicz, J.A. McCammon, S.T. Wlodek, M.K. Gilson, Simulation of charge-mutant acetylcholinesterases, Biochemistry 34 (1995) 4211–4219.
[10] H.-X. Zhou, J.M. Briggs, J.A. McCammon, A 240-fold electrostatic rate-enhancement for acetylcholinesterase-substrate binding can be predicted by the potential within the active site, J. Am. Chem. Soc. 118 (1996) 13069–13070.
[11] Z. Radic, P. Kirchoff, D.M. Quinn, J.A. McCammon, P. Taylor, Electrostatic influence on the kinetics of ligand binding to acetylcholinesterase. Distinctions between active center ligands and fasciculin, J. Biol. Chem. 272 (1997) 23265–23277.
[12] M.K. Gilson, T.P. Straatsma, J.A. McCammon, D.R. Ripoll, C.H. Faerman, P.H. Axelsen, I. Silman, J.L. Sussman, Open 'back door' in a molecular dynamics simulation of acetylcholinesterase, Science 263 (1994) 1276–1278.
[13] A. Shafferman, A. Ordentlich, D. Barak, C. Kronman, R. Ber, T. Bino, N. Ariel, R. Osman, B. Velan, Electrostatic attraction by surface charge does not contribute to the catalytic efficiency of acetylcholinesterase, EMBO J. 13 (1994) 3448–3455.
[14] D.R. Ripoll, C.H. Faerman, R. Gillilan, I. Silman, J.L. Sussman, Electrostatic properties of human acetylcholinesterase, in: D.M. Quinn, A.S. Balasubramanian, B.P. Doctor, P. Taylor (Eds.), Enzymes of the Cholinesterase Family, Plenum, New York, 1995, pp. 67–70.
[15] H.K. Nair, D.M. Quinn, *m*-Alkyl α,α,α-trifluoroacetophenones: a new class of potent transition state analog inhibitors of acetylcholinesterase, Bioorg. Med. Chem. Lett. 3 (1993) 2619–2622.
[16] H.K. Nair, K. Lee, D.M. Quinn, *m*-(*N*,*N*,*N*-trimethylammonio)trifluoroacetophenone: a femtomolar inhibitor of acetylcholinesterase, J. Am. Chem. Soc. 115 (1993) 9939–9941.
[17] Z. Radic, G. Gibney, S. Kawamoto, K. MacPhee-Quigley, C. Bongiorno, P. Taylor, Expression of recombinant acetylcholinesterase in a baculovirus system: kinetic properties of glutamate 199 mutants, Biochemistry 31 (1992) 9760–9767.
[18] D.C. Vellom, Z. Radic, Y. Li, N.A. Pickering, S. Camp, P. Taylor, Amino acid residues controlling acetylcholinesterase and butyrylcholinesterase specificity, Biochemistry 32 (1993) 12–17.
[19] Z. Radic, N.A. Pickering, D.C. Vellom, S. Camp, P. Taylor, Three distinct domains in the cholinesterase molecule confer selectivity for acetyl- and butrylcholinesterase inhibitors, Biochemistry 32 (1993) 12074–12084.
[20] A. Shafferman, B Velan, A. Ordentlich, C. Kronman, H. Grosfeld, M. Leitner, Y. Flashner, S. Cohen, D. Barak, N. Ariel, Substrate inhibition of acetylcholinesterase: residues affecting signal transduction from the surface to the catalytic center, EMBO J. 11 (1992) 3561–3568.
[21] A. Ordentlich, C. Kronman, D. Barak, D. Stein, N. Ariel, D. Marcus, B. Velan, A. Shafferman, Engineering resistance to 'aging' of phosphylated human acetylcholinesterase. Role of hydrogen bond network in the active center, FEBS Lett. 334 (1993) 215–220.
[22] G.L. Ellman, K.D. Courtney, V. Andres, Jr., R.M. Featherstone, A new and rapid colorimetric determination of acetylcholinesterase activity, Biochem. Pharmacol. 7 (1961) 88–95.
[23] H.K. Nair, J. Seravalli, T. Arbuckle, D.M. Quinn, Molecular recognition in acetylcholinesterase catalysis: free-energy correlations for substrate turnover and inhibition by trifluoro ketone transition state analogs, Biochemistry 33 (1994) 8566–8576.
[24] D.M. Quinn, J. Seravalli, H.K. Nair, R.A. Medhekar, B. Husseini, Z. Radic, D.C. Vellom, N. Pickering, P. Taylor, The function of electrostatics in acetylcholinesterase catalysis, in: D.M. Quinn, A.S. Balasubramanian, B.P. Doctor, P. Taylor (Eds.), Enzymes of the Cholinesterase Family, Plenum, New York, 1995, pp. 203–208.
[25] B.R. Brooks, R.E. Bruccoleri, B.D. Olafson, D.J. States, S. Swaminathan, M. Karplus, CHARMM: a program for macromolecular energy, minimization, and dynamics calculations, J. Comp. Chem. 4 (1983) 187–217.
[26] M. Harel, D.M. Quinn, H.K. Nair, I. Silman, J.L. Sussman, The X-ray structure of a transition state analog complex reveals the molecular origins of the catalytic power and substrate specificity of acetylcholinesterase, J. Am. Chem. Soc. 118 (1996) 2340–2346.

[27] B.S. Zhorov, N.N. Shestakova, E.V. Rozengart, Determination of productive conformation of acetylcholinesterase substrates using molecular mechanics, Quant. Struct.-Act. Relat. 10 (1991) 205–210.